Supplementary Materials for manuscript "**China's clean air and climate policies help improve farmers' incomes and reduce socioeconomic inequity via mitigating ozone pollution**" authored by Mao et al. (2026)

GCHP model simulation. GEOS-Chem, a global 3D chemical transport model (CTM) equipped with a detailed gas-phase mechanism of NO_x-VOC-O_3 chemistry, is widely used to estimate regional or global surface O_3 concentrations. A high-performance capability for GEOS-Chem (GCHP), with the identical source code for physical and chemical mechanisms with GEOS-Chem, was developed to take advantage of massively parallel computing architectures [1,2]. In this study, we used GCHP version 13.2.1 with full tropospheric chemistry, driven by assimilated meteorological data from Modern-Era Retrospective Analysis for Research and Applications, Version 2 (MERRA2), to estimate surface O_3 at a horizontal resolution of C48 (~2.0° latitude × 2.5° longitude) and 72 vertical layers. Dry deposition for gases and aerosols is diagnosed based on the resistance-in-series scheme [3] in the base version. Biogenic VOC emissions are computed by the Model of Emissions of Gases and Aerosols from Nature (MEGAN) v2.1 [4], which is embedded in GCHP. Biomass burning emissions are from the Global Fire Emissions Database (GFED4) inventory [5]. The global monthly anthropogenic emissions of BC, OC, NH_3, NO_x, SO_2 and NMVOCs are from the Community Emissions Data System (CEDS) [6], while the anthropogenic emissions in China are obtained from the Multiresolution Emission Inventory (MEIC; http://meicmodel.org.cn/).

Our baseline simulation [CTRL] was performed representative of 2015, and three additional experiments with mitigation controls were conducted to examine the long-term individual and synergistic effects of clean air (CA) and carbon neutrality (CN) policies on crop production by 2060: CA_2060, CN_2060, and CA_CN_2060. The future projected anthropogenic emissions in China are from the Dynamic Projection model for Emissions in China Version 1.2 (DPEC v1.2) developed by Tsinghua University to track China's future greenhouse gases and air pollutant emissions from 2020 to 2060 under a wide range of socioeconomic, climate, and pollution control policies. All simulations were performed for the same meteorological conditions of 2015 after an additional spin-up period of 6 months.

LightGBM model. LightGBM is a machine learning (ML) algorithm based on the gradient-boosting

decision tree [7], which has a high training efficiency and lower memory footprint and is thus suitable for processing massive high-dimensional data. In this study, we used to the LightGBM model to correct the bias of the GCHP-simulated O_3 fields for the present-day control scenario [CTRL].

To fully utilize the potential of big data and the integrative capabilities of ML, multiple-source datasets were used for model training and validation, including O_3 observations, anthropogenic emissions, meteorology, land use, topography and other auxiliary data. Hourly surface O_3 observations ($\mu g\ m^{-3}$) from 2016 to 2018 were obtained from the China National Environmental Monitoring Center Network (https://air.cnemc.cn:18007/) established by the Ministry of Ecology and Environment of China. A total of 1016 sites were finally selected after removing sites with missing data rates greater than 5%. Also, the abnormal values greater than 500 $\mu g\ m^{-3}$ were deleted. The monthly historical (2015–2018) anthropogenic emissions of O_3 precursor gases, including NO_x, NMVOCs and CO were obtained from the same input datasets used by GCHP [8]. Hourly reanalysis data for meteorological variables were obtained from the fifth-generation European Centre for Medium-Range Weather Forecasts (ECMWF) reanalysis dataset (ERA5) with a spatial resolution of 0.25° × 0.25° (https://cds.climate.copernicus.eu/). The national land-use data with a spatial resolution of 30 m × 30 m for 2015 were provided by Yang and Huang [9]. Nationwide topography data at a resolution of 1 km × 1 km were provided by the Chinese Academy of Sciences (https://www.resdc.cn/data.aspx?DATAID=123), sourced from the latest Shuttle Radar Topography Mission (SRTM) v4.1 dataset produced by NASA. The 1 km × 1 km gridded real gross domestic product (GDP) for 2015 is provided by Chen et. al [10]. The population density data with a high-precision spatial resolution of 30 arcseconds in 2015 is provided by Liu et. al [11]. When predicting the gridded O_3 concentrations with the trained model, predictor variables at different spatial resolutions were all regridded to the same resolution of 0.25° × 0.25°, consistent with the ERA5 meteorological fields.

A timescale of 2 years strike a good balance between computational burden and model accuracy as training the model with 1 year or more of data only results in marginal improvements in model performances [12]. Here the LightGBM model was trained with samples over 2016–2017 and the 2018 data independent of the model training process was used for model validation. The ozone observations from 2016 to 2018 used for validation were obtained from the China National Environmental Monitoring Center Network (https://air.cnemc.cn:18007/). A total of 1016 sites were selected after deleting the missing and abnormal data. The overall coefficient of determination (R^2) values of the

hybrid approach and GCHP model are 0.67 and 0.42 at the hourly level. Bias-corrected ozone concentrations show lower root mean square errors (RMSEs) than GCHP-simulated concentrations, reduced from 36.3 to 25.8 $\mu g\, m^{-3}$ (**Figure S9**). The results suggest that the hybrid approach, by integrating process-based CTM outputs and multi-source datasets at higher resolutions, can deliver more accurate ozone predictions. Comparable performance on both the training and test datasets (**Figure S10**) indicates no obvious overfitting. This generalization capacity justifies its use in bias-correcting the GCHP-simulated ozone fields for the [CTRL] scenario.

Figures

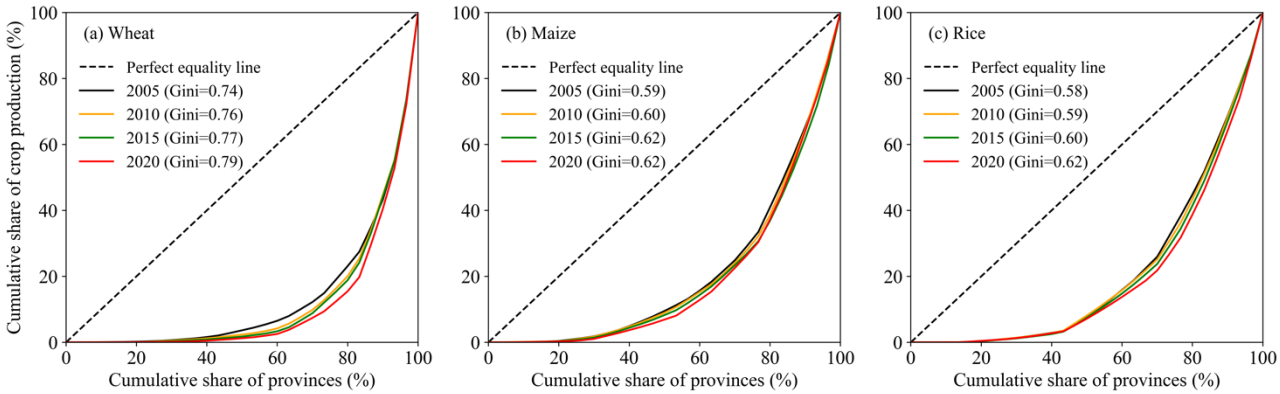

Figure S1. The Lorenz curve and Gini coefficient for the production of three major crops from 2005 to 2020: (a) wheat, (b) maize, and (c) rice.

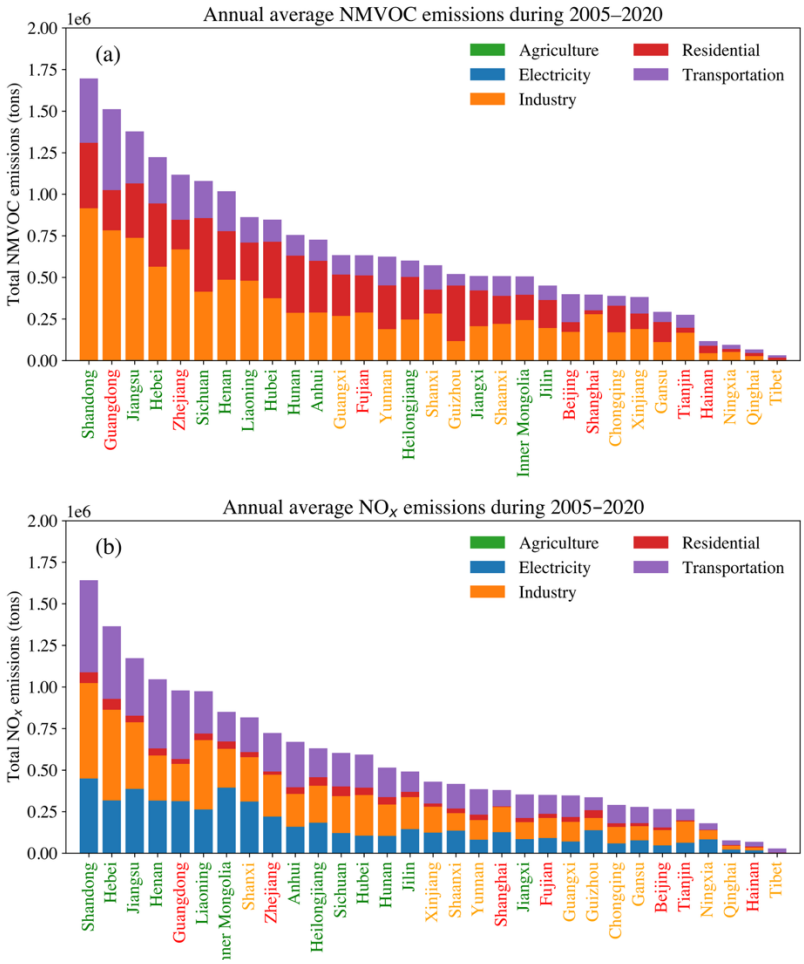

Figure S2. Annual average emissions of (a) NMVOC and (b) NO_x across provinces from 2005 to 2020 by different emission sectors.

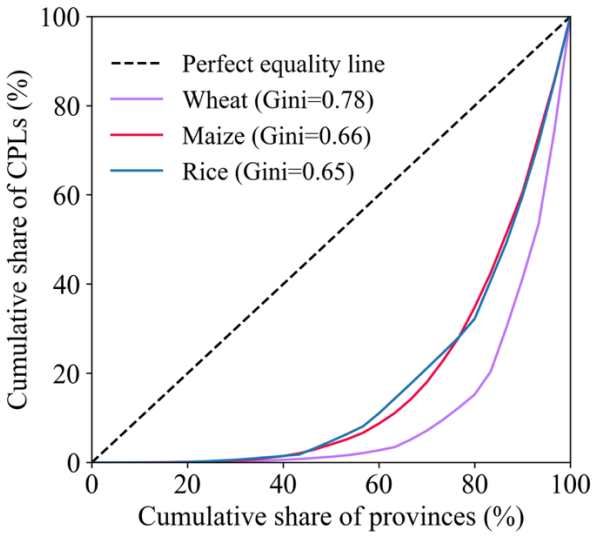

Figure S3. Lorenz curve and Gini coefficient for present-day crop production losses (CPLs) for wheat, maize, and rice.

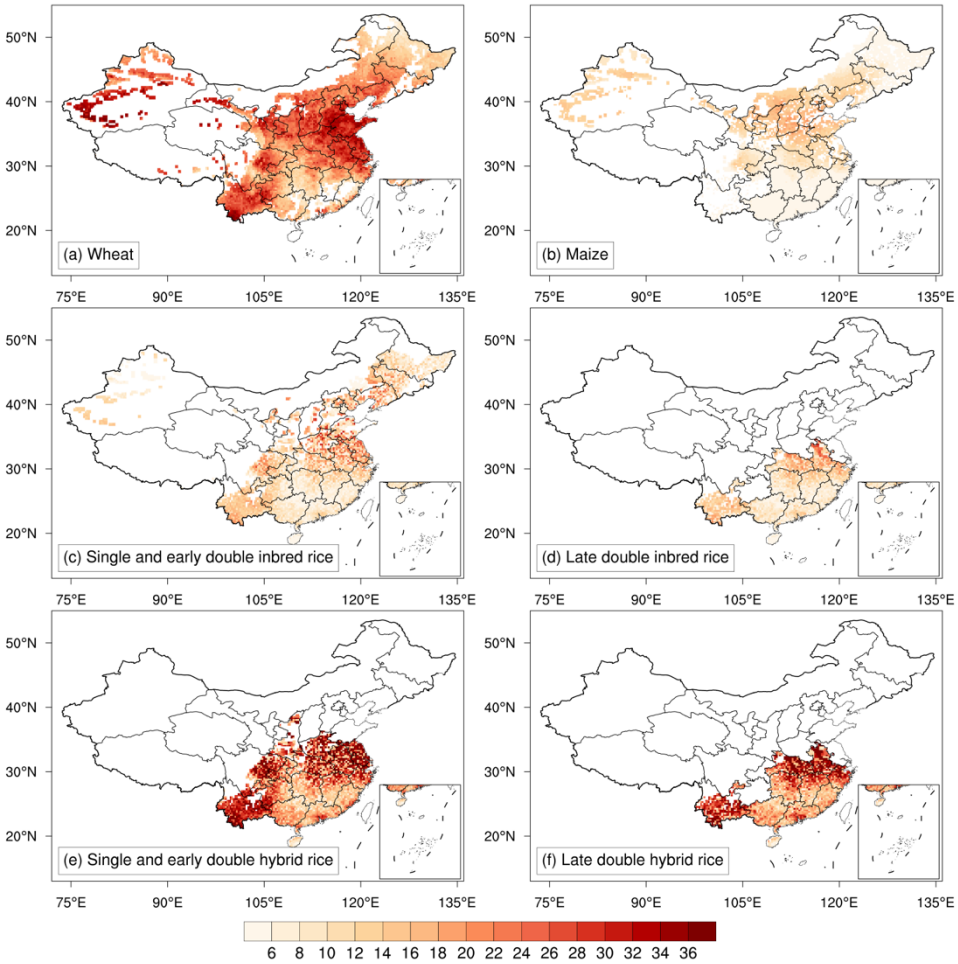

Figure S4. Present-day relative yield losses (RYLs, %) for different crops in China, calculated from Asian-specific exposure–RY relationships: (a) wheat, (b) maize, (c) single and early double crop inbred rice, (d) late double crop inbred rice, (e) single and early double crop hybrid rice, and (f) late double crop hybrid rice.

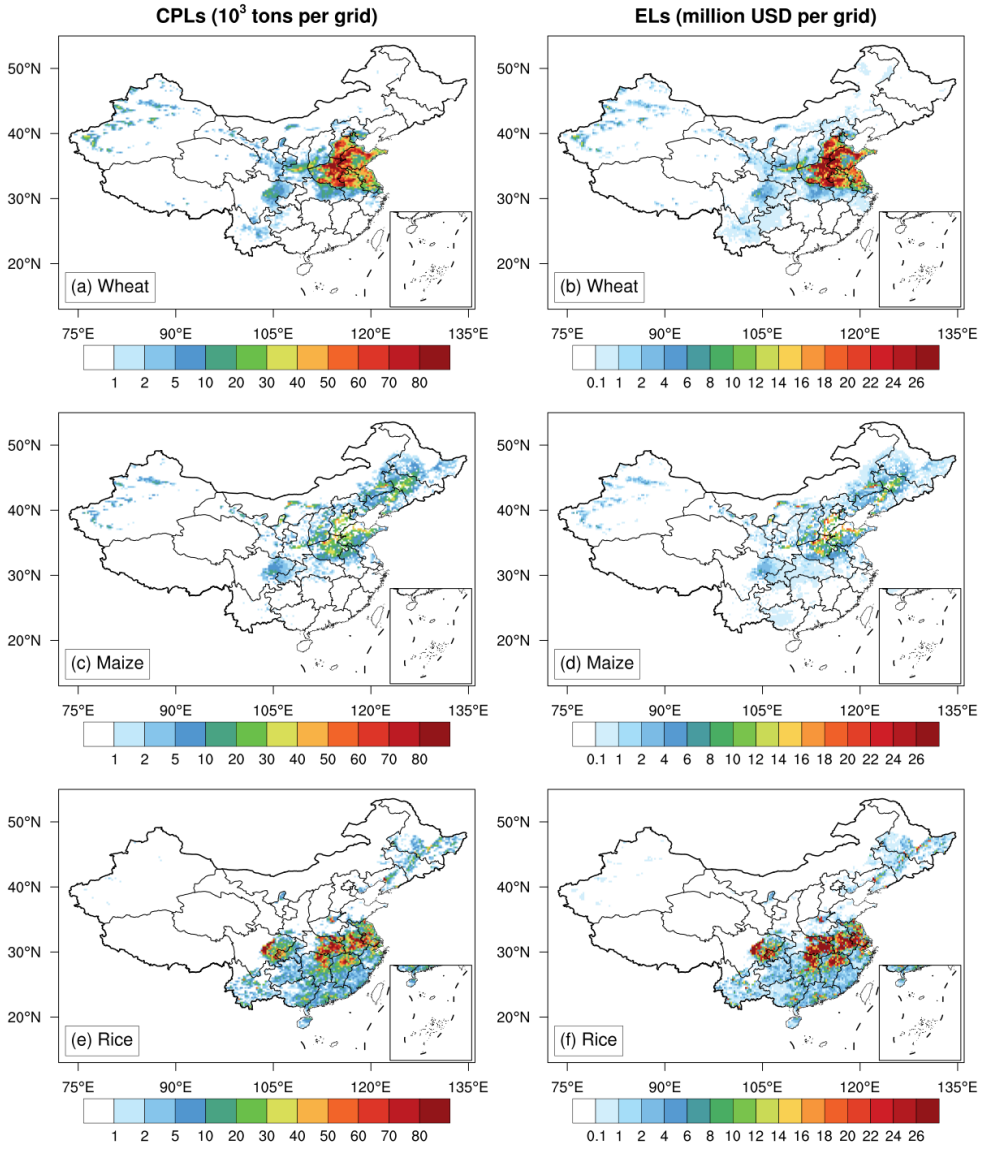

Figure S5. Ozone-induced crop production losses (CPLs; in thousand metric tons per 0.25°×0.25° grid cell) for: (a) wheat, (c) maize, and (e) rice, and the corresponding economic losses (ELs; in million USD per 0.25°×0.25° grid cell) for (b) wheat, (d) maize, and (f) rice.

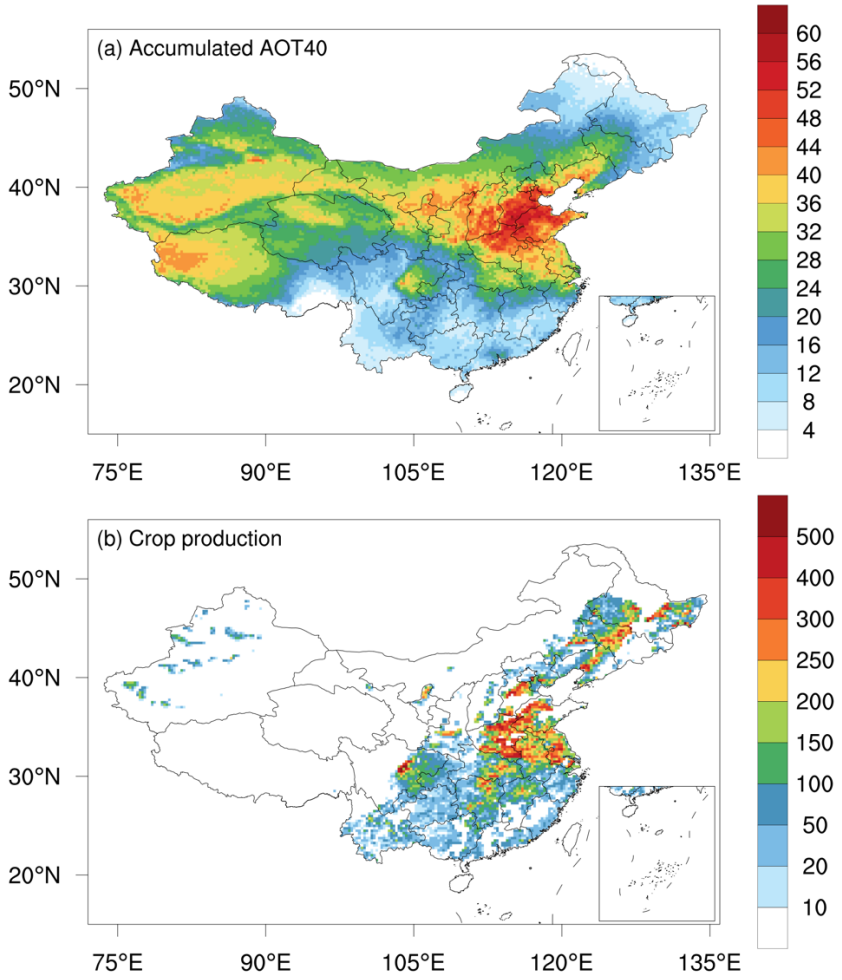

Figure S6. (a) Accumulated AOT40 (10^3 ppb) during the major growing season (April–September) in 2015; (b) total production of the three major crops (in thousand metric tons per 0.25° × 0.25° grid cell) in 2015.

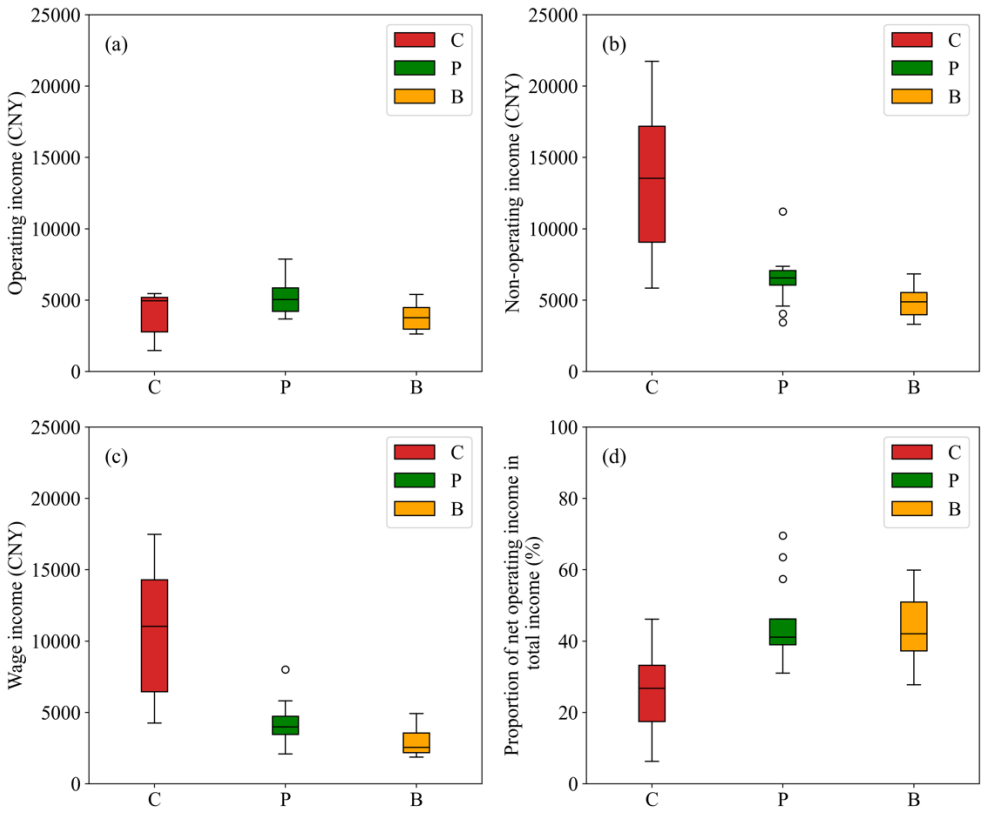

Figure S7. Sources of rural residents' disposable income: (a) net operating income, (b) non-operating income, (c) wage income, and (d) the proportion of net operating income in total income. According to the National Bureau of Statistics of China (NBSC), disposable income comprises four components: wage income, net operating income, net property income, and net transfer income. Net operating income refers to the net income obtained by households or household members from production and business activities, such as farmers earning income from agricultural production. Wage income refers to the total labor remuneration and various benefits obtained by employed individuals through different means, including wages and benefits from employment with organizations or individuals, as well as earnings from freelance work, part-time jobs, and occasional labor.

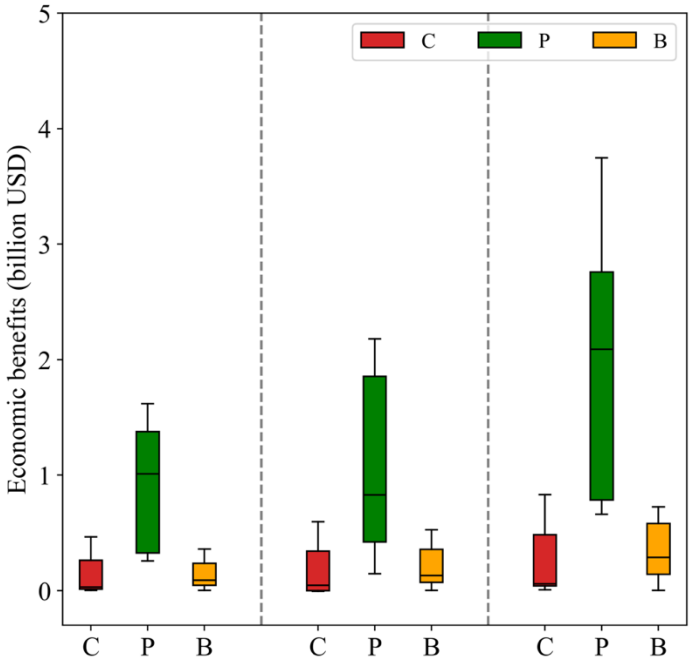

Figure S8. Boxplot of provincial economic benefits due to reduced CPLs under various policy scenarios across food functional region.

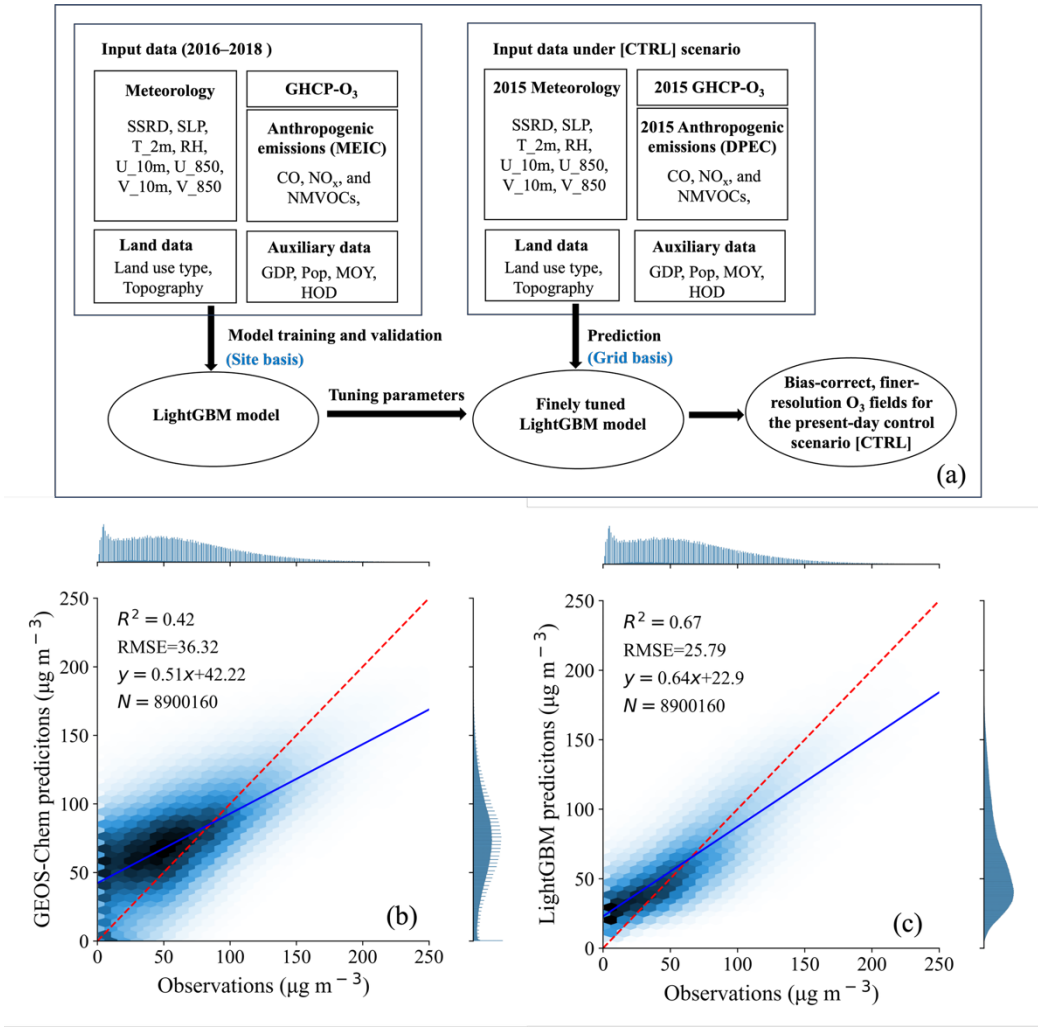

Figure S9. (a) Flowchart illustrating the hybrid approach for predicting present-day and future ozone concentrations under various scenarios, with abbreviations and detailed information of variables provided in **Table S1**. Density scatterplots and linear regression statistics of ozone predictions vs. observations for 2018 independent of the process of model training: (b) GCHP-simulated hourly ozone vs. observations, and (c) bias-corrected hourly ozone vs. observations. The model results are sampled at the same site locations. The dashed red line represents the 1:1 line, and the solid blue line shows the orthogonal regression line of best fit. R^2 is the coefficient of determination, RMSE is the root mean square error, and N is the number of data points. The original unit of GCHP-simulated ozone is parts per billion (ppb), which was converted to $\mu g\, m^{-3}$ assuming a constant temperature of 25 °C and pressure of 1013.25 hPa (1 $\mu g\, m^{-3}$ is approximately 0.5 ppb) for comparison with observations.

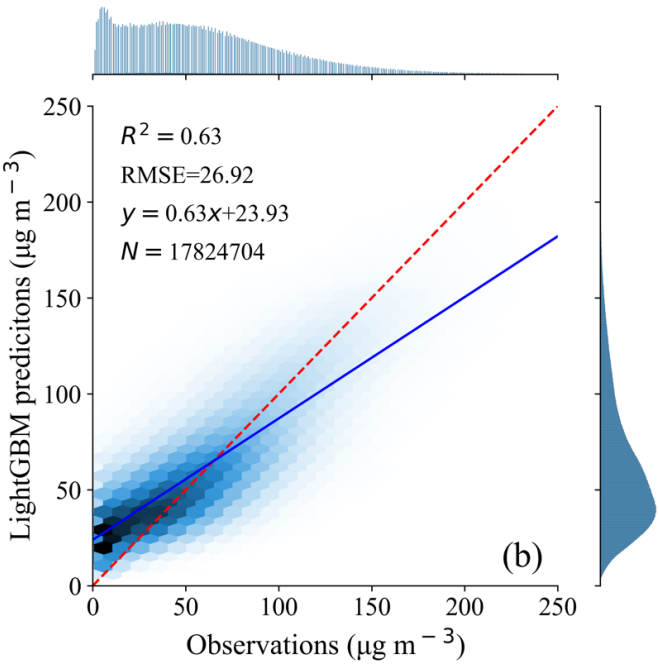

117

118 **Figure S10.** Density scatterplots and linear regression statistics of LightGBM O_3 predictions (μg m^{-3})
119 compared with observations for 2016–2017 training data. The dashed red line represents the 1:1 line,
120 and the solid blue line shows the orthogonal regression line of best fit. R^2 is the coefficient of
121 determination, RMSE is the root mean square error, and N is the number of data points.

122

Tables

Table S1. Provincial production of three major grain crops (Mt) in 2015 and corresponding types: producing areas (P), balanced production areas (B) and consuming areas (C).

Provinces	Wheat	Maize	Rice	Total	Type
Beijing	0.11	0.49	0.00	0.6	C
Tianjin	0.60	1.07	0.11	1.78	C
Hebei	14.35	16.70	0.55	31.6	P
Shanxi	2.71	8.63	0.00	11.34	B
Inner Mongolia	1.58	22.51	0.53	24.62	P
Liaoning	0.03	14.04	4.68	18.75	P
Jilin	0.00	28.06	6.30	34.36	P
Heilongjiang	0.22	35.44	22.00	57.66	P
Shanghai	0.20	0.02	0.84	1.06	C
Jiangsu	11.74	2.52	19.52	33.78	P
Zhejiang	0.35	0.31	5.78	6.44	C
Anhui	14.11	4.96	14.59	33.66	P
Fujian	0.01	0.21	4.85	5.07	C
Jiangxi	0.03	0.13	20.27	20.43	P
Shandong	23.47	20.51	0.95	44.93	P
Henan	35.01	18.54	5.32	58.87	P
Hubei	4.21	3.33	18.11	25.65	P
Hunan	0.09	1.89	26.45	28.43	P
Guangdong	0.00	0.78	10.88	11.66	C
Guangxi	0.01	2.81	11.38	14.2	B
Hainan	0.00	0.00	1.53	1.53	C
Chongqing	0.23	2.60	5.06	7.89	B
Sichuan	4.26	7.66	15.53	27.45	P
Guizhou	0.62	3.24	4.18	8.04	B
Yunnan	0.91	7.47	6.60	14.98	B

Tibet	0.23	0.01	0.00	0.24	B
Shaanxi	4.58	5.43	0.92	10.93	B
Gansu	2.81	5.77	0.03	8.61	B
Qinghai	0.34	0.19	0.00	0.53	B
Ningxia	0.40	2.27	0.61	3.28	B
Xinjiang	6.98	7.05	0.65	14.68	B

126 **Table S2.** Provincial crop production losses (CPLs; Mt) of three major grain crops and total economic
127 losses (ELs; billion USD) in 2015.

Provinces	**Wheat CPLs**	**Maize CPLs**	**Rice CPLs**	**Total CPLs**	**Total ELs**
Beijing	0.04	0.02	0.00	0.06	0.02
Tianjin	0.27	0.15	0.01	0.43	0.17
Hebei	6.43	2.12	0.10	8.65	3.41
Shanxi	1.05	1.61	0.00	2.66	1.09
Inner Mongolia	0.39	2.96	0.08	3.43	1.47
Liaoning	0.01	1.81	0.90	2.72	1.24
Jilin	0.00	2.17	0.81	2.98	1.35
Heilongjiang	0.03	1.24	1.88	3.15	1.50
Shanghai	0.08	0.00	0.15	0.23	0.10
Jiangsu	5.29	0.26	4.81	10.36	4.56
Zhejiang	0.13	0.02	1.65	1.8	0.89
Anhui	5.82	0.73	6.70	13.25	5.92
Fujian	0.00	0.00	0.87	0.87	0.44
Jiangxi	0.01	0.01	4.86	4.88	2.47
Shandong	11.21	2.98	0.17	14.36	5.63
Henan	13.58	3.38	2.35	19.31	7.81
Hubei	1.29	0.27	8.24	9.8	4.78
Hunan	0.02	0.10	5.85	5.97	3.01
Guangdong	0.00	0.02	1.99	2.01	1.01
Guangxi	0.00	0.10	1.94	2.04	1.03

Hainan	0.00	0.00	0.17	0.17	0.09
Chongqing	0.06	0.21	1.88	2.15	1.07
Sichuan	1.46	0.90	7.79	10.15	4.89
Guizhou	0.17	0.03	0.97	1.17	0.57
Yunnan	0.33	0.04	1.93	2.3	1.12
Tibet	0.08	0.00	0.00	0.08	0.03
Shaanxi	1.56	0.56	0.19	2.31	0.93
Gansu	0.89	0.49	0.00	1.38	0.55
Qinghai	0.10	0.00	0.00	0.1	0.04
Ningxia	0.15	0.34	0.10	0.59	0.25
Xinjiang	2.73	1.13	0.06	3.92	1.56

128 **Table S3.** Provincial CPLs (Mt) for wheat under different scenarios.

Province	**CA_2060**	**CN_2060**	**CA_CN_2060**
Beijing	0.04	0.05	0.04
Tianjin	0.29	0.33	0.25
Hebei	6.39	7.46	5.36
Shanxi	0.87	0.85	0.53
Inner Mongolia	0.36	0.34	0.28
Liaoning	0.01	0.01	0.01
Jilin	0.00	0.00	0.00
Heilongjiang	0.03	0.03	0.02
Shanghai	0.07	0.08	0.05
Jiangsu	4.51	4.74	2.79
Zhejiang	0.08	0.07	0.04
Anhui	4.41	4.25	2.39
Fujian	0.00	0.00	0.00
Jiangxi	0.00	0.00	0.00
Shandong	10.24	12.24	7.85
Henan	11.28	11.98	7.49

Hubei	0.94	0.81	0.46
Hunan	0.01	0.01	0.00
Guangdong	0.00	0.00	0.00
Guangxi	0.00	0.00	0.00
Hainan	0.00	0.00	0.00
Chongqing	0.04	0.03	0.02
Sichuan	1.02	0.79	0.55
Guizhou	0.12	0.10	0.07
Yunnan	0.31	0.30	0.26
Tibet	0.08	0.08	0.07
Shaanxi	1.16	0.98	0.57
Gansu	0.70	0.63	0.42
Qinghai	0.09	0.09	0.07
Ningxia	0.12	0.11	0.08
Xinjiang	2.55	2.44	2.05

129 **Table S4.** Provincial CPLs (Mt) for maize under different scenarios.

Province	**CA_2060**	**CN_2060**	**CA_CN_2060**
Beijing	0.01	0.01	0.01
Tianjin	0.11	0.10	0.06
Hebei	1.51	1.30	0.68
Shanxi	1.08	0.82	0.41
Inner Mongolia	2.24	1.83	1.23
Liaoning	1.22	1.00	0.48
Jilin	1.39	1.20	0.58
Heilongjiang	0.75	0.66	0.34
Shanghai	0.00	0.00	0.00
Jiangsu	0.16	0.11	0.04
Zhejiang	0.01	0.01	0.00
Anhui	0.43	0.26	0.09

Fujian	0.00	0.00	0.00
Jiangxi	0.01	0.00	0.00
Shandong	2.04	1.54	0.74
Henan	2.19	1.52	0.71
Hubei	0.16	0.09	0.04
Hunan	0.05	0.03	0.01
Guangdong	0.00	0.00	0.00
Guangxi	0.06	0.05	0.04
Hainan	0.00	0.00	0.00
Chongqing	0.14	0.07	0.03
Sichuan	0.53	0.33	0.17
Guizhou	0.02	0.01	0.00
Yunnan	0.02	0.02	0.01
Tibet	0.00	0.00	0.00
Shaanxi	0.37	0.27	0.13
Gansu	0.35	0.30	0.21
Qinghai	0.00	0.00	0.00
Ningxia	0.24	0.21	0.13
Xinjiang	1.00	0.97	0.82

130 **Table S5.** Provincial CPLs (Mt) for rice under different scenarios.

Province	**CA_2060**	**CN_2060**	**CA_CN_2060**
Beijing	0.00	0.00	0.00
Tianjin	0.01	0.01	0.01
Hebei	0.09	0.10	0.08
Shanxi	0.00	0.00	0.00
Inner Mongolia	0.07	0.07	0.06
Liaoning	0.83	0.86	0.67
Jilin	0.70	0.69	0.49
Heilongjiang	1.64	1.61	1.22

Shanghai	0.14	0.16	0.11
Jiangsu	3.98	4.00	2.58
Zhejiang	1.00	0.80	0.43
Anhui	4.31	3.55	1.94
Fujian	0.37	0.24	0.11
Jiangxi	2.55	1.76	0.82
Shandong	0.15	0.17	0.12
Henan	1.73	1.62	0.99
Hubei	5.47	4.20	2.35
Hunan	3.49	2.52	1.26
Guangdong	0.94	0.68	0.30
Guangxi	1.21	0.88	0.59
Hainan	0.11	0.08	0.06
Chongqing	1.34	0.87	0.53
Sichuan	5.22	3.99	2.74
Guizhou	0.68	0.53	0.35
Yunnan	1.83	1.76	1.61
Tibet	0.00	0.00	0.00
Shaanxi	0.12	0.09	0.05
Gansu	0.00	0.00	0.00
Qinghai	0.00	0.00	0.00
Ningxia	0.09	0.08	0.06
Xinjiang	0.06	0.06	0.05

131 **Table S6.** Provincial ELs (billion USD) under different scenarios.

Province	**CA_2060**	**CN_2060**	**CA_CN_2060**
Beijing	0.02	0.02	0.02
Tianjin	0.16	0.18	0.13
Hebei	3.13	3.45	2.37
Shanxi	0.80	0.68	0.38

Inner Mongolia	1.14	0.96	0.67
Liaoning	0.95	0.88	0.55
Jilin	0.95	0.87	0.50
Heilongjiang	1.16	1.11	0.77
Shanghai	0.10	0.11	0.08
Jiangsu	3.80	3.88	2.39
Zhejiang	0.54	0.44	0.24
Anhui	4.05	3.52	1.93
Fujian	0.19	0.12	0.06
Jiangxi	1.30	0.90	0.42
Shandong	4.85	5.40	3.36
Henan	6.11	6.04	3.65
Hubei	3.20	2.47	1.39
Hunan	1.79	1.29	0.64
Guangdong	0.48	0.35	0.15
Guangxi	0.64	0.47	0.32
Hainan	0.06	0.04	0.03
Chongqing	0.76	0.48	0.29
Sichuan	3.26	2.47	1.67
Guizhou	0.40	0.31	0.20
Yunnan	1.05	1.01	0.92
Tibet	0.03	0.03	0.03
Shaanxi	0.66	0.54	0.30
Gansu	0.42	0.37	0.25
Qinghai	0.04	0.04	0.03
Ningxia	0.20	0.18	0.12
Xinjiang	1.43	1.37	1.16

132 **Table S7.** Detailed information of variables used for LightGBM model training in this study. ERA5:
133 the fifth-generation European Centre for Medium-Range Weather Forecasts (ECMWF) reanalysis

dataset; MEIC: the Multiresolution Emission Inventory; SRTM: Shuttle Radar Topography Mission.

Dataset type	Variable	Description	Spatial resolution	Temporal resolution	Time period	Data source
O_3	GCHP_O_3	Near-surface hourly O_3	2.0°×2.5°	Hourly	2016-2018	GCHP simulation
Anthropogenic emissions	NO_x	Nitric oxide from anthropogenic sources	0.25°×0.25°	Monthly	2016-2018	MEIC
	CO	Carbon monoxide from anthropogenic sources				
	NMVOC	Non-methane volatile organic compounds from biogenic sources				
Meteorology	T_2m	Air temperature at 2 m	0.25°×0.25°	Hourly	2016-2018	ERA5
	SLP	Sea level pressure				
	U_10m	Zonal wind at 10 m				
	U_850	Zonal wind at 850 hPa				
	V_10m	Meridional wind at 10 m				
	V_850	Meridional wind at 850 hPa				
	SSRD	Incoming shortwave radiation at the surface				
	RH	Relative humidity				

Land data	LU	Land use type	30 m × 30 m	–	2016-2018	[9]
	TOPO	Digital elevation	1 km × 1 km	–	–	SRTM
Auxiliary data	MOY	Month of the year	–	–	–	–
	DOH	Hour of the day	–	–	–	–
	GDP	Gross domestic product	1 km × 1 km	–	2016-2018	[10]
	Pop	Pop density	30 arc × 30 arc	–	2016-2018	[11]

Table S8. Summary of all simulations with GCHP models.

Scenario	Abbreviation	Anthropogenic emissions	Meteorological condition
Present-day	CTRL	Emissions in 2015	2015
Clean air	CA_2060	Emissions in 2060 with additional air pollution control under the SSP1 assumption	2015
Carbon neutrality	CN_2060	Emissions in 2060 with additional climatic constraints under the SSP1 assumption	2015
Clean air + carbon neutrality	CA_CN_2060	Emissions in 2060 with integrated air pollution and climatic controls under the SSP1 assumption	2015

Table S9. Statistical relationships between relative yield (RY) and AOT40 from Feng [13]. RY is defined as the ratio of ozone-affected yield to the unaffected yield at zero ozone exposure.

Crop	**Dose-yield relationship**
Maize	$RY = 1 - S\,[AOT40 + (40 - x) * 1.08 - (20.22 - 0.01264\,x^2) / (1 + 0.207\,AOT40 - 0.0001293\,x^2\,AOT40)] / [1 - S\,(22.98 - 1.08\,x + 0.01264\,x^2)]$, $S = 0.0068$ and $x = 40.0$
Wheat	$RY = 1 - S\,[AOT40 + (40 - x) * 1.08 - (20.22 - 0.01264\,x^2) / (1 + 0.207\,AOT40 - 0.0001293\,x^2\,AOT40)] / [1 - S\,(22.98 - 1.08\,x + 0.01264\,x^2)]$, $S = 0.0161$ and $x = 26.5$

Rice	$RY = 1 - S\,[AOT40 + (40 - x) * 1.08 - (20.22 - 0.01264\,x^2) / (1 + 0.207\,AOT40 - 0.0001293\,x^2\,AOT40)] / [1 - S\,(22.98 - 1.08x + 0.01264\,x^2)]$, $S = 0.0071$ for inbred cultivars, $S = 0.0145$ for hybrid cultivars, and $x = 19.4$ for both inbred and hybrid cultivars

138

139

References

1. Eastham, S. D. *et al.* GEOS-Chem High Performance (GCHP v11-02c): a next-generation implementation of the GEOS-Chem chemical transport model for massively parallel applications. *Geosci Model Dev* **11**, 2941–2953 (2018).
2. Martin, R. V. *et al.* Improved advection, resolution, performance, and community access in the new generation (version 13) of the high-performance GEOS-Chem global atmospheric chemistry model (GCHP). *Geosci. Model Dev.* **15**, 8731–8748 (2022).
3. Wesely, M. L. Parameterization of surface resistances to gaseous dry deposition in regional-scale numerical models. *Atmospheric Environ. 1967* **23**, 1293–1304 (1989).
4. Guenther, A. B. *et al.* The Model of Emissions of Gases and Aerosols from Nature version 2.1 (MEGAN2.1): an extended and updated framework for modeling biogenic emissions. *Geosci Model Dev* **5**, 1471–1492 (2012).
5. van der Werf, G. R. *et al.* Global fire emissions estimates during 1997–2016. *Earth Syst Sci Data* **9**, 697–720 (2017).
6. Hoesly, R. M. *et al.* Historical (1750–2014) anthropogenic emissions of reactive gases and aerosols from the Community Emissions Data System (CEDS). *Geosci. Model Dev.* **11**, 369–408 (2018).
7. Chen, T. & Guestrin, C. XGBoost: A Scalable Tree Boosting System. (2016).
8. Li, H. *et al.* Ozone Pollution in China Affected by Climate Change in a Carbon Neutral Future as Predicted by a Process-Based Interpretable Machine Learning Method. *Geophys. Res. Lett.* **51**, e2024GL109520 (2024).
9. Yang, J. & Huang, X. The 30 m annual land cover dataset and its dynamics in China from 1990 to 2019. *Earth Syst. Sci. Data* **13**, 3907–3925 (2021).

10. Chen, J. *et al.* Global 1 km × 1 km gridded revised real gross domestic product and electricity consumption during 1992–2019 based on calibrated nighttime light data. *Sci. Data* **9**, 202 (2022).
11. Liu, L., Cao, X., Li, S. & Jie, N. A 31-year (1990–2020) global gridded population dataset generated by cluster analysis and statistical learning. *Sci. Data* **11**, 124 (2024).
12. Mao, J. *et al.* Multidecadal ozone trends in China and implications for human health and crop yields: a hybrid approach combining a chemical transport model and machine learning. *Atmos Chem Phys* **24**, 345–366 (2024).
13. Feng, Z. *et al.* Ozone pollution threatens the production of major staple crops in East Asia. *Nat. Food* **3**, 47–56 (2022).